Detailed analysis of tracking detectors for SAMURAI08 experiment

S. Koyama,[*1,*2] H. Otsu,[*2] for SAMURAI08 collaboration

We performed an experiment at SAMURAI to search for α-cluster levels in ^{16}C.[1)] The levels were populated by bombarding a ^{16}C secondary beam on a liquid He target. The excitation energies were reconstructed from the invariant mass of the $^{16}C^* \to {}^{12}Be + {}^4He$ decay channel by measuring their four momenta. The four momenta were deduced from timing measurements and the tracking of drift chambers (DCs). For these DCs, the tracking efficiency and position resolution depend on the energy loss in the detector, which depends on the element number (Z) of penetrating fragments. In order to determine the four momenta accurately, the parameters for tracking should be separately optimized for each Z.

Figure 1 shows a particle identification (PID) plot of reaction products measured using the plastic scintillator array HODF and HODP.[2)] Note that 1 scintillator out of 32 of the array on which the secondary beam directly hits with an intensity of 2×10^5 is excluded.

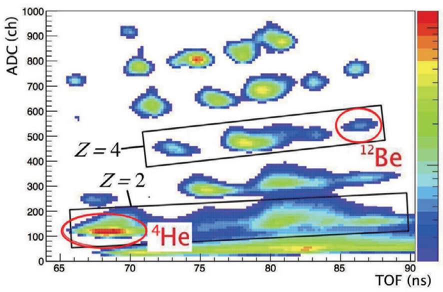

Fig. 1. PID plot of reaction products. The vertical axis shows the mean light output and the horizontal axis shows the time of flight (TOF) between the plastic scintillator placed upstream of the target and HODF and HODP.

DCs consist of more than 3 planes with different kinds of wire orientations. FDC2,[2)] which was placed downstream of the SAMURAI magnet[2)] ($B = 2.3$ T at the center), has 6 X (vertical, 0°), 4 U (+30°) and 4 V (−30°) planes. The drift length on each plane is measured and the trajectories of fragments for one axial direction, $x = a_0 + a_1 z$, are reconstructed by fitting a linear function, where x is the position orthogonal to the beam line, a_0 and a_1 are linear fitting parameters and z is the position along the beam line. The x positions of fragments in the k-th plane of a DC x_k are deduced from the time-to-digital converter (TDC) spectrum with a space-time conversion (STC) function, which converts time information to drift length. The STC function is first obtained by integrating the TDC spectrum and is corrected in response to the result of tracking.

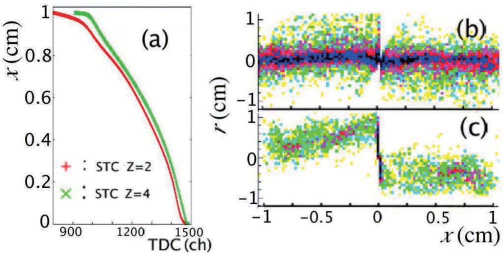

Fig. 2. (a) The optimized STC functions for $Z = 2$ (red) and $Z = 4$ (green) fragments. (b) $x_k - r_k$ correlation with the optimized STC function. (c) $x_k - r_k$ correlation with an unoptimized STC function.

Figure 2 (a) shows the two STC functions optimized for $Z = 2$ and $Z = 4$ fragments. The difference between the two functions is clear. The residue r_k is defined as $r_k = x_k - x'_k$, where $x'_k = a_0 + a_1 z_k$ and z_k is the z position of the k-th plane. Figs. 2 (b) and (c) show how $x_k - r_k$ correlation changes when a different STC function is applied for tracking. The positions are well reconstructed when the optimized STC function is applied (Fig. 2 (b)) while they systematically deviate from the case in which an inappropriate STC function is applied (Fig. 2 (b)).

The position resolution of the k-th plane of a DC Δx_k can be evaluated using the standard deviation of the residue of the plane Δr_k as follows:

$$\Delta r_k = \sqrt{1 - \frac{S_{zz} - 2S_z z_k + S_1 z_k^2}{D}}\Delta x, \tag{1}$$

where $S_1 = \sum_k 1, S_z = \sum_k z_k, S_{zz} = \sum_k z_k^2$, and $D = S_1 S_{zz} - S_z^2$. It is assumed that Δx_k has the same value Δx in the same wire-oriented planes of a DC to deduce Eq. 1. Table 1 summarizes the position resolutions of X, U, and V planes with the optimized STC function for each Z. The position resolution of FDC2 is 120 μm[2)] for $Z = 6$. Note that the value of the high voltage (2.4 kV) is not optimized for one Z to measure fragments with different Z in this experiment.

Table 1. Resolution of each plane of FDC2

Wire orientation	Resolution (μm) $Z = 2$	Resolution (μm) $Z = 4$
X	342	309
U	255	195
V	257	199

References
1) H. Otsu et. al.: RIKEN Accel. Prog. Rep. 47, xx (2014).
2) T. Kobayashi et. al.: Nucl. Instrum. Meth. B 317 (2013).

*1 Department of Physics, University of Tokyo
*2 RIKEN Nishina Center